This paper is a Post-Print version (i.e. final draft post-refereeing).
For access to Publisher's version,please access
DOI: 10.1109/RO-MAN50785.2021.9515392 .

A variable admittance controller for human-robot manipulation of large inertia objects

Antonis Sidiropoulos, Theodora Kastritsi, Dimitrios Papageorgiou, Zoe Doulgeri

***Abstract*— In this work, the problem of cooperative human-robot manipulation of an object with large inertia is addressed, considering the availability of a kinematically controlled industrial robot. In particular, a variable admittance control scheme is proposed, where the damping is adjusted based on the power transmitted from the human to the robot, with the aim of minimizing the energy injected by the human while also allowing her/him to have control over the task. The proposed approach is evaluated via a human-in-the-loop setup and compared to a generic variable damping state-of-the-art method. The proposed approach is shown to achieve significant reduction of the human's effort and minimization of unintended overshoots and oscillations, which may deteriorate the user's feeling of control over the task.**

I. Introduction

The field of robotics has exhibited remarkable progress over the past few decades. The vision of having robots work alongside humans is slowly beginning to materialize. Especially in industrial environments, this collaboration between human-robot can significantly improve productivity and efficiency. Humans can bring experience, knowledge, perception and understanding for the proper execution of each task and robots can reduce fatigue and increase human capabilities in terms of strength, speed and accuracy. Thus, the physical human-robot interaction (pHRI) can significantly increase the overall performance by fully exploiting their complementary abilities to complete the task.

Collaborative human-robot object transfer has been recently proposed for reducing the human's effort as much as possible. When no full prior knowledge of the task is available, the user communicates her/his intention haptically, i.e. via physical guidance. Although the problem of collaborative object transfer is extensively studied in the literature, the problem of handling an object with high inertia is not explicitly addressed. Such cases are commonly found in industry, for instance in car assembly production lines, where workers have to manipulate cumbersome and heavy parts for visual inspection and/or pre-assembly. A specific example of such a case is the human-robot collaborative manipulation of a windshield utilizing an industrial robotic manipulator, depicted in Fig.1.

Most of the available industrial robotic manipulators are kinematically controlled, accepting joint position/velocity commands. Hence, in cooperative manipulation of objects, an admittance control scheme is utilized, to generate reference velocities based on measurements of the external forces applied to the object by the user. In general, admittance control schemes render a specific target impedance model, which is typically selected to be a second order linear dynamical system, i.e. a mass-spring-damper, involving target inertia $\boldsymbol{M}$, damping $\boldsymbol{D}$ and stiffness $\boldsymbol{K}$. In cases where the human should be able to physically move the robot freely, the target impedance model does not involve a stiffness term. Assuming an ideally kinematically controlled robot, the reference trajectory is perfectly tracked and the system under admittance control with constant impedance parameters is passive. However, it is proven that in the realistic case, the trajectory tracking performance imposes a lower limit on the selection range of the target inertia parameter $\boldsymbol{M}$ [1]–[3]. In particular, the minimum allowed target inertia value depends on the real inertia of the physical plant, in order for the overall system to be passive. Specifically, [1] states that the target inertia should be roughly larger than half the inertia of the plant. This means that a plant, which involves an object with relatively large inertia, imposes a relatively high lower limit on the selection of the target inertia parameter of the admittance controller.

In general, the value of target damping $\boldsymbol{D}$ plays a crucial role on the response of the system during the physical interaction with the human. In particular, given the specific dynamics of the human-robot coupled system and considering a constant target inertia, fixed to its minimum value to minimize the human effort, relatively small values of $\boldsymbol{D}$ will decrease the physical effort of the human. However,

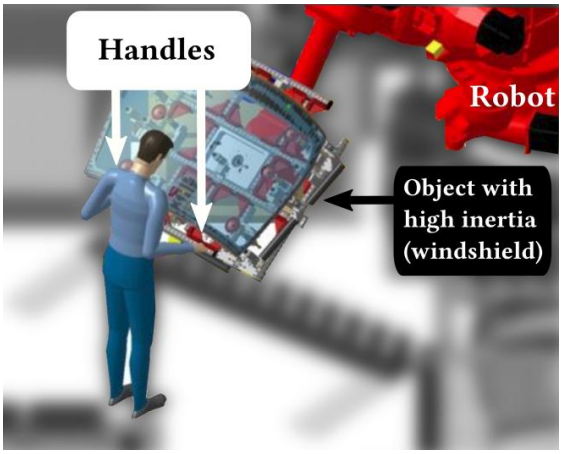

Fig. 1: An industrial Example.
Image taken from https://cordis.europa.eu/project/id/820767/results

The research leading to these results has received funding by the EU Horizon 2020 Research and Innovation Programme under grant agreement No 820767, project CoLLaboratE.

All authors are with the Aristotle University of Thessaloniki, Department of Electrical and Computer Engineering, Thessaloniki 54124, Greece.

in our case, the allowed target inertia is large, inducing high momentum and therefore a low value of $\boldsymbol{D}$ may yield overshoots and oscillations during the interaction, which in turn will deteriorate the human's feeling of control over the task and may jeopardize her/his safety. On the other hand, a relatively large value of $\boldsymbol{D}$ will make the interaction more controllable for the human, at the cost however of increased effort.

In this work, we aim at both reducing the human's physical effort, quantified by the energy transmitted from the human to the robot, and enhancing the human's feeling of control over the task, as reflected and quantified by the energy transmitted on the opposite direction, i.e. from the robot to the human. Notice that the two objectives are contradictory w.r.t. to the selection of $\boldsymbol{D}$, as explained above, and therefore one cannot select a constant damping parameter in order to fulfill them simultaneously. This necessitates the utilization of a variable damping parameter. Our contribution is the implementation of a variable admittance control scheme for manipulating large objects with high inertia, where the damping is adjusted based on the power transmitted from the human to the robot, with the aim of minimizing the energy injected by the human while also allowing her/him to have control over the task. The proposed approach is compared with other admittance control schemes in human-in-the-loop simulations involving the manipulation of a large object with high inertia.

II. Related literature

In the literature, physical human robot interaction is achieved by designing a desired relation between external force and position, the so called impedance model. This can be done either via an impedance controller [4], i.e. by sending torque commands to the robot based on its kinematic state, or by an admittance control [5], [6], i.e. by sending kinematic commands to the robot based on the external force measurements. Impedance control is considered to be more appropriate for robots with low inertia and friction, since the user will inevitably feel these forces, while admittance control is utilized mostly in cases of kinematically controlled robots, accepting motion commands, e.g. common industrial robots.

In the past decades, several studies have proposed different methods to determine the parameters of the impedance model in order to improve the physical human-robot interaction and make the cooperation transparent. A survey of the methods that involve adaptation of the impedance parameters can be found in [7]. R. Ikeura together with his team proposed methods for designing the robot's admittance model based on the human impedance characteristics, which were identified through a collaborative task between two humans [8]. They deduced that the human damping coefficient varies in time and depends on the velocity of the interaction. In [9] the desired damping was switched between two discrete preset values, depending on the velocity of the end-effector. Some years later the same research team designed a variable damping coefficient based on a cost function [10], whose type however may differ depending on the duration of the task and distance traveled, making the method task-specific. In [11] a variable admittance control is proposed as a means of coordination between a human and a robot to share a load, which is adjusted according to the force exerted on the robotic arm. When the force changes, the compliance will increase or decrease accordingly. Duchaine et al. [12] used the time derivative of the force to adjust the damping factor, in order to ensure the smooth tracking of the human movement by the robot in a pick-and-place and a drawing task.

Ficuciello et al. [13] proposed a method for varying the impedance parameters based on the velocity of the end-effector in a generic pHRI task with a cobot. In particular, the damping is selected to be a decreasing function of the velocity, implying a relatively high damping for small velocities and a relatively small damping for high velocities. However, the collaborative manipulation of a object with large inertia could induce high momentum, which means that a variable damping depending on the velocity of the interaction will not necessarily decrease overshoots and/or oscillations. Dimeas et al. [14] proposed a fuzzy inference system that relies on the measured velocity and the force applied by the operator to on-line adjust the damping of the admittance controller in a pick-and-place task, with the aim to yield a minimum jerk interaction. However, the latter method requires prior knowledge of the task motion for the training, which is quite restrictive and task-specific. Grafakos et al. [15] proposed a variable admittance model, in which the damping is adjusted based on the operator's muscle activation measured by EMG, utilizing a switch function between two discrete damping values.

In all the aforementioned works, the problem of handling an object with high inertia is not explicitly addressed; a case which is commonly found in industrial applications. In [3], [16], which are not covered by [7], an admittance controller is utilized for the cooperative manipulation of a heavy object, which adjusts the target inertia and damping matrices depending on the acceleration. However, the paper tackles only one of the objectives of the current paper, as only the problem of enhancing the user's feeling of control over the task is addressed, i.e. the so called "intuitiveness of interaction", without taking into account the physical effort of the user.

III. Proposed Approach

Consider a n-dof industrial robotic manipulator, which grasps and holds a large rigid object with high inertia, and let $\boldsymbol{q} \in \mathbb{R}^n$ be the vector of its joint variables. Due to the size of the object, we consider the case in which the human interacts with it using both hands, via two handles equipped with 6-D force/torque sensors (Fig.1). Let the frame $\{o\}$ be placed at the center of mass (CoM) of the object and frames $\{1\}$, $\{2\}$ be placed at the force/torque sensors of the left and right handle respectively. Due to the rigidity of the object and the grasping, the poses of these frames with respect to the world frame $\{w\}$, which is located at the robot's base, are

functions of the joint variables of the robot and their relative poses are constant. Let $\boldsymbol{x}_o(\boldsymbol{q}), \boldsymbol{x}_1(\boldsymbol{q}), \boldsymbol{x}_2(\boldsymbol{q}) \in SE(3)$ be the generalized poses of the object and the sensors (1 and 2) respectively, with respect to $\{w\}$, which involve their position $\boldsymbol{p}_i(\boldsymbol{q}) \in \mathbb{R}^3$ and their orientation $\boldsymbol{R}_i(\boldsymbol{q}) \in SO(3)$, where $i = \{o, 1, 2\}$.

Let $\boldsymbol{V}_i = [\boldsymbol{v}_i^\intercal \ \boldsymbol{\omega}_i^\intercal]^\intercal \in \mathbb{R}^6$ be the generalized body velocity of frame $\{i\}$, $i = \{o, 1, 2\}$, with $\boldsymbol{v}_i, \boldsymbol{\omega}_i \in \mathbb{R}^3$ being the translational and angular body velocities of the frame respectively. The mapping between the generalized body velocities of the frames and the robot's joint velocities is given by:

$$\boldsymbol{V}_i = {}^i\boldsymbol{J}_i(\boldsymbol{q})\dot{\boldsymbol{q}}, \ i = \{o, 1, 2\}, \tag{1}$$

where ${}^i\boldsymbol{J}_i(\boldsymbol{q}) \in \mathbb{R}^{6,\times n}$ is the Jacobian for frame $\{i\}$.

Let, $\boldsymbol{F}_1(t) = [\boldsymbol{f}_1(t)^\intercal \ \boldsymbol{\tau}_1(t)^\intercal]^\intercal$ and $\boldsymbol{F}_2(t) = [\boldsymbol{f}_2(t)^\intercal \ \boldsymbol{\tau}_2(t)^\intercal]^\intercal \in \mathbb{R}^6$ be the generalized forces measured by the 6-D F/T sensors of the first and second handle respectively, expressed in the respective sensor frames, i.e. $\{1\}$ and $\{2\}$. Considering a kinematically controlled robot, we utilize a Cartesian admittance control scheme for providing the robot with compliance properties, by rendering a target impedance model, which is based on the measured external forces $\boldsymbol{F}_1$ and $\boldsymbol{F}_2$. The target impedance model is defined for the object, w.r.t. to $\{o\}$, and it is given by:

$$\boldsymbol{M}\dot{\boldsymbol{V}}_o + \boldsymbol{D}\boldsymbol{V}_o = \boldsymbol{F}_o, \tag{2}$$

where

$$\boldsymbol{F}_o = \boldsymbol{R}_o^\intercal \left[\boldsymbol{G}(\boldsymbol{p}_1 - \boldsymbol{p}_o)\boldsymbol{R}_1\boldsymbol{F}_1 + \boldsymbol{G}(\boldsymbol{p}_2 - \boldsymbol{p}_o)\boldsymbol{R}_2\boldsymbol{F}_2\right], \tag{3}$$

with

$$\boldsymbol{G}(\boldsymbol{p}) = \begin{bmatrix} \boldsymbol{I}_3 & \boldsymbol{0}_3 \\ \boldsymbol{S}(\boldsymbol{p}) & \boldsymbol{I}_3 \end{bmatrix} \in \mathbb{R}^{6\times 6}, \tag{4}$$

and $\boldsymbol{S}(.) : \mathbb{R}^3 \to \mathbb{R}^{3\times 3}$ denoting the skew symmetric matrix mapping. In order to apply the aforementioned admittance control, one has to online integrate (2) to obtain $\boldsymbol{V}_o$ and then map it to the joint space utilizing the inverse of (1).

Assuming an ideally kinematically controlled robot, the closed loop system is completely described by (2) and is passive with respect to $\boldsymbol{V}_o$ for any constant positive definite matrices $\boldsymbol{M}, \boldsymbol{D}$, under the exertion of the external force $\boldsymbol{F}_o$. However, considering a realistic non-perfect trajectory tracking, the minimum allowed value of $\boldsymbol{M}$, for retaining passivity, depends on the inertia of the physical plant. In our case, the plant involves the object with high inertia, which imposes a relatively high lower limit on the selection of $\boldsymbol{M}$. In the light of this limitation, we utilize a constant portion of the known real inertia of the object and therefore we select:

$$\boldsymbol{M} = \alpha \begin{bmatrix} m_o\boldsymbol{I}_3 & \boldsymbol{0}_3 \\ \boldsymbol{0}_3 & \boldsymbol{M}_o \end{bmatrix}, \tag{5}$$

where $\alpha \in (0, 1)$ is the constant portion of the inertia of the real plant, $m_o \in \mathbb{R}_{>0}$ is the mass of the object and $\boldsymbol{M}_o \in \mathbb{R}^3$ its constant diagonal inertia tensor expressed in its own frame $\{o\}$. Drawing our inspiration from [13], we propose the following law for the variation of the damping parameter, which depends on the power transmitted from the human to the robot during the interaction:

$$\boldsymbol{D}(P^+) = \underline{\boldsymbol{D}} + (\overline{\boldsymbol{D}} - \underline{\boldsymbol{D}})e^{-\lambda P^+}, \tag{6}$$

where

$$P^+ \triangleq \max\left(0, \ \boldsymbol{V}_o^\intercal \boldsymbol{F}_o\right) \in \mathbb{R}_{\geq 0} \tag{7}$$

is the power transmitted from the human to the robot, $\underline{\boldsymbol{D}}, \overline{\boldsymbol{D}} \in \mathbb{R}^{3\times 3}$ are constant diagonal matrices representing the minimum and maximum damping values respectively and $\lambda \in \mathbb{R}_{>0}$ is a constant tunable parameter affecting the sensitivity of the damping to changes of the power.

The rationale behind the last term of (6) is based on the idea that the human intention for motion is reflected by the transmission of power from her/him to the system. In particular, when the object held by the robot is physically guided by the human, i.e. the direction of motion is towards the force applied by the human, the user will experience low damping, since this indicates her/his intention to move the object. On the other hand, when the velocity of the object is opposite to the force applied by the human, the motion of the robot will be maximally damped based on (6), due to the fact that P^+ will be zero. The aforementioned properties are able to fulfill our objectives, namely the minimization of the physical effort and the enhancement of the human's feeling of control over the task, as also demonstrated in the following section.

Theorem 1: The closed loop system (2) is passive with respect to the velocity of the object $\boldsymbol{V}_o$, under the exertion of the force applied to the object $\boldsymbol{F}_o$.

Proof: For the system (2) consider the following storage function:

$$L = \frac{1}{2}\boldsymbol{V}_o^\intercal \boldsymbol{M}\boldsymbol{V}_o. \tag{8}$$

The time derivative of (8), after substituting $\boldsymbol{M}\dot{\boldsymbol{V}}_o$ from (2), $\boldsymbol{D}$ from (6), is given by:

$$\dot{L} = -\boldsymbol{V}_o^\intercal \left[\underline{\boldsymbol{D}} + (\overline{\boldsymbol{D}} - \underline{\boldsymbol{D}})e^{-\lambda P^+}\right]\boldsymbol{V}_o + \boldsymbol{V}_o^\intercal \boldsymbol{F}_o. \tag{9}$$

Given $(\overline{\boldsymbol{D}} - \underline{\boldsymbol{D}})e^{-\lambda P^+} > 0, \ \forall P^+ \in \mathbb{R}_{\geq 0}$, the following inequality is derived from (9):

$$\dot{L} < -\boldsymbol{V}_o^\intercal \underline{\boldsymbol{D}}\boldsymbol{V}_o + \boldsymbol{V}_o^\intercal \boldsymbol{F}_o. \tag{10}$$

Inequality (10) implies the system's passivity with respect to object velocity $\boldsymbol{V}_o$, under the exertion of $\boldsymbol{F}_o$. ■

IV. Validation through human-in-the-loop simulations

The proposed approach is validated via human-in-the-loop simulations. The simulation setup is presented in Fig. 2b. The virtual environment is displayed through a computer screen with the object and the robotic manipulator that holds it, visualized with RViz, as shown in Fig. 2a. An ideally kinematically controlled KUKA LWR4+ robot is used in the virtual environment holding an object of 160kg, with inertia tensor equal to $\boldsymbol{M}_o = \text{diag}(8.56, 1.66, 10.16) Nms^2/rad$. The portion of the real inertia utilized for the target inertia of

the admittance controller is $\alpha = 0.5$. The distance between the two handles is 0.44m. For simulating the physical interaction of the human with the object, two UR5e robots are utilized, with handles fixed at their end-effectos, emulating the handles of the virtual object. The generalized forces applied by the human are measured by the F/T sensors of each UR5e and used for integrating on-line (2), based on the calculated force (3), to yield the desired trajectory of the object $\boldsymbol{V}_o$. The object's velocity $\boldsymbol{V}_o$ is then mapped to the KUKA robot's joint space utilizing the inverse of (1). To provide haptic feedback to the user, the velocity of each virtual handle is calculated based on $\boldsymbol{V}_o$, and then sent as command to the corresponding velocity controlled UR5e manipulator. Thus, the relative pose of the UR5e robots' end-effectors remains constant, while the pose of each UR5e handle faithfully reflects the pose of the corresponding object handle fixed on the virtual visualized object, giving to the user the sense of manipulating a real heavy object.

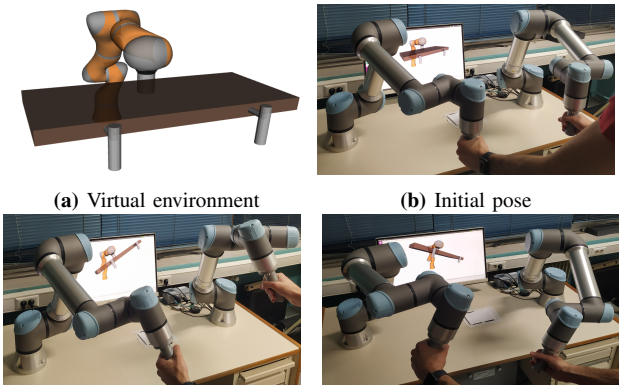

(a) Virtual environment **(b)** Initial pose

(c) First target pose **(d)** Second target pose

Fig. 2: human-in-the-loop simulation setup.

The task is to move the object and bring it approximately to the pose shown in Fig. 2c, halt momentarily (e.g. to inspect the object) and then move it to the pose depicted in Fig. 2d. Notice that the task involves relatively small displacement in translation and larger ones for orientation, as the object has to be rotated principally around the axis normal to the computer screen. The proposed approach is implemented by applying the admittance controller (2) with (5) and (6) for two different values of λ, namely $\lambda = \{2,\ 10\}$, to assess the performance variability with different values of this parameter. We also compared our method with the variable damping based on the velocity norm, proposed in [13], with $\lambda = 15$. In both cases, the minimum damping was set to $\underline{\boldsymbol{D}} = \text{diag}(20\boldsymbol{I}_3,\ 0.2\boldsymbol{I}_3)$ and the maximum to $\overline{\boldsymbol{D}} = \text{diag}(350\boldsymbol{I}_3,\ 10\boldsymbol{I}_3)$. For further comparison, we also examine the case of having a constant damping. Specifically, we conducted experiments with the minimum, maximum and mean value of the aforementioned min/max damping values.

We conducted simulations with ten different participants. Each participant executed the task six times, once for each of the aforementioned damping cases. The order of execution for these six methods was randomly generated for each participant based on a uniform distribution. The employed evaluation metrics are: a) the energy transferred by the human to the robot, calculated by the integral of the power from (7), i.e. $E^+ \triangleq \int_0^T P^+ dt$, with T denoting the interaction duration, which reflects the effort of the human; b) the energy transferred from the robot to the human, calculated by the integral of the negative power accordingly, i.e. $E^- \triangleq |\int_0^T P^- dt|$, where $P^- \triangleq \min(0,\ \boldsymbol{V}_o^\intercal \boldsymbol{F}_o)$, which quantifies the robot's opposition to the human's forces.

Typical results from one participant are presented in Table I and Fig. 3-5. In Table I, the energy values E^+ and E^- from each simulation are given, for each one of the six damping cases. Normalized values, w.r.t the maximum energy (6.843J) of the participant, are given in parentheses. It is clearly visible that the physical effort, quantified by E^+, when utilizing a constant mean ($\boldsymbol{D}_{mean}$) or high damping ($\boldsymbol{D}_{max}$) is significantly larger than the rest of the cases. It is also worth noticing that the velocity-based variable damping ($\boldsymbol{D}_{vel}$) yields similar physical effort to the proposed one (with $\lambda = 10$). However, regarding the robot's opposition to human forces, reflected by E^-, it is evident that the proposed approach ($\boldsymbol{D}_{pow}$) significantly outperforms both the utilization of a low constant damping ($\boldsymbol{D}_{min}$) and the velocity-based variable damping ($\boldsymbol{D}_{vel}$). In particular, E^- is more than 4 times less than in the other two cases. Lastly, notice that the effort is less when utilizing $\lambda = 10$ compared to $\lambda = 2$, which is reasonable due to the fact that, for larger values of λ, the damping reduction is more sensitive to changes of the transmitted power.

Fig. 3 and 4 show the results for comparing the proposed method with the velocity-based one. In particular, Fig. 3 depicts the power for the proposed approach ($\boldsymbol{D}_{pow}$), for the two values of λ, compared to the velocity-based damping approach ($\boldsymbol{D}_{vel}$). Notice the relatively similar power transfer from the human to the robot between the proposed approach (P^+: cyan line), for $\lambda = 10$, and the velocity-based approach (P^+: red line). However, the power transferred from the robot to the human with the proposed approach (P^-: blue line) is significantly lower than the one with the velocity-based adaptation (P^-: dark red line), which means that the human perceived greater opposition with the velocity-based approach. This is due to the fact that the velocity-based approach significantly reduces the damping when the object has a relatively large velocity, and consequently a motion can occur even if the human does not apply any forces given the high momentum. It is also interesting to note that oscillations occur in the power transmission during the reaching and stabilization of the object at each pose, with the velocity-based approach. This fact implies that the human faced difficulty to stabilize the object. Fig. 4 depicts the power transferred between the human and the robot and the damping co-efficient variation with the proposed approach ($\lambda = 10$), compared to the velocity-based approach. It is evident that, with the velocity-based damping, there are time periods, e.g. at $t \approx 1.6 - 2.5$ and $t \approx 5.9 - 6.8$ (right column of Fig. 4), during which the robot opposes the human's

intention, signified by the magnitude of the negative power, while the damping remains at its lowest values. On the other hand, the magnitude of this opposition is negligible with the proposed approach , since the damping is instantly increased when any opposition of the robot to the human's intention occurs, e.g. at $t \approx 1.6 - 2.2$ and $t \approx 4 - 5.2$ (left column of Fig. 4).

Fig. 5 depicts the power with the proposed approach ($\boldsymbol{D}_{pow}$), for the two values of λ, compared to the case of utilizing a constant damping equal to the mean value of $\underline{\boldsymbol{D}}$ and $\overline{\boldsymbol{D}}$ ($\boldsymbol{D}_{mean}$). In the bottom row of Fig. 5, for $\lambda = 10$, a small oscillation occurs in both cases in the power transmission when reaching each pose. This similarity is also reflected by the values of E^- between $\boldsymbol{D}_{pow}$ and $\boldsymbol{D}_{mean}$ of Table I. Nevertheless, the power transmission from human to robot is significantly reduced with the proposed approach, compared to the utilization of the constant mean damping; the effort is approximately half for $\lambda = 2$ and approximately $1/3$ for $\lambda = 10$. This observation becomes even more clear by examining the energy transmission E^+ in Table I.

TABLE I: Energy transferred between the participant and the robot with different damping selections. The values within the parenthesis correspond to the normalized values, i.e. divided by 6.843.

Damping	E^+	E^-
$\boldsymbol{D}_{pow}(\lambda = 2)$	3.149 (**0.46**)	0.015 (**0.00**)
$\boldsymbol{D}_{pow}(\lambda = 10)$	2.226 (**0.33**)	0.217 (**0.03**)
$\boldsymbol{D}_{vel}$	2.176 (**0.32**)	2.321 (**0.34**)
$\boldsymbol{D}_{mean}$	4.781 (**0.70**)	0.318 (**0.05**)
$\boldsymbol{D}_{min}$	2.076 (**0.30**)	2.081 (**0.30**)
$\boldsymbol{D}_{max}$	6.843 (**1.00**)	0.028 (**0.00**)

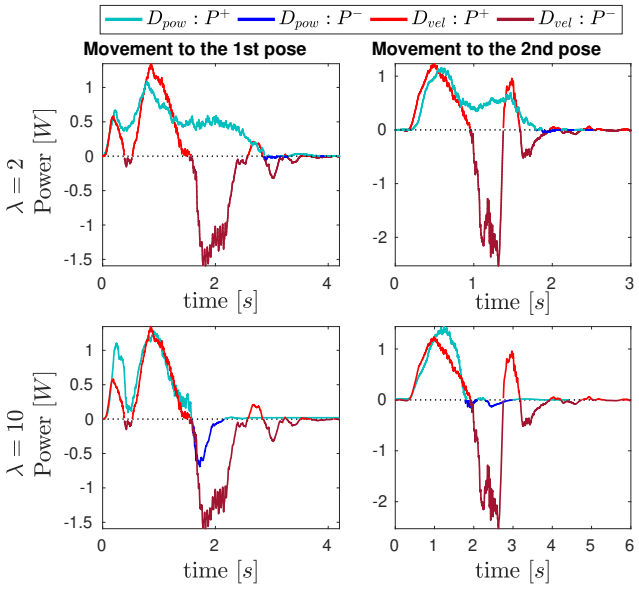

Fig. 3: Power transmission between the participant and the robot for adapting the damping based on the power (cyan and blue lines) and on the velocity (red and dark red lines), for $\lambda = 2$ (first row) and $\lambda = 10$ (second row).

The statistical results obtained from the entire sample of the 10 subjects are in line with the conclusions drawn from

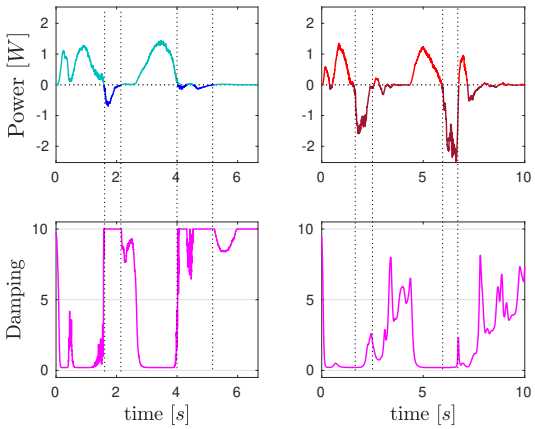

Fig. 4: Damping adaptation for the orientation with the power based case ($\lambda = 10$) on the first column, compared to the velocity based case on the right column.

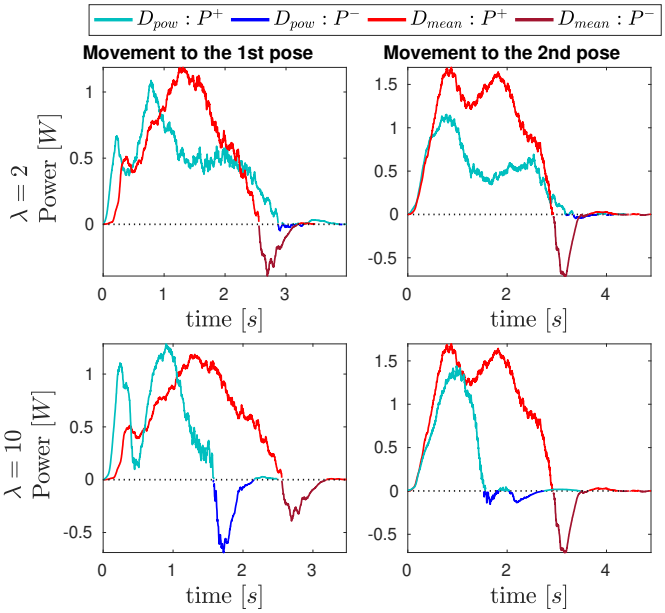

Fig. 5: Power transmission between the participant and the robot for adapting the damping based on the power (cyan and blue lines) and with the (constant) mean damping, for for $\lambda = 2$ (first row) and $\lambda = 10$ (second row).

these typical results. A paired t-test between the proposed method and each one of the other methods is performed. Specifically, in Fig.6, the boxplots of E^+ and E^- are depicted for all subjects. Blue areas in Fig. 6 correspond to methods which are outperformed by the proposed method, i.e. significant reduction of the mean value with $p < 0.05$ (t-test). Furthermore, in Table II, the difference of the mean values are presented, where red color represents a significant increase of the mean value, while blue color represents a significant reduction of the mean value when employing the proposed method; the non-colored cells corresponds to a statistically insignificant difference, based on the t-test. From the statistical evaluation, it is evident that the proposed method outperforms the $\boldsymbol{D}_{mean}$ and $\boldsymbol{D}_{max}$ regarding E^+

as also found in the aforementioned typical results. Furthermore, $\boldsymbol{D}_{vel}$ and $\boldsymbol{D}_{min}$ perform worse regarding E^-, which is in accordance with the results from a single participant.

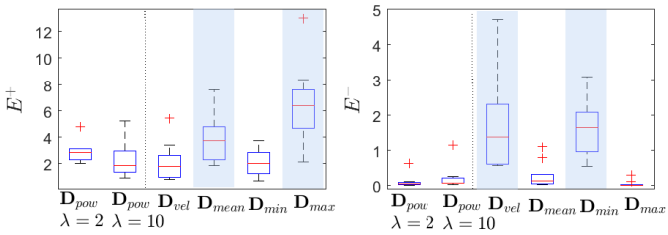

Fig. 6: Boxplots of E^+ and E^- for 10 participants. Blue color denotes a significant improvement (based on the t-test) achieved by the proposed method compared to the corresponding one.

TABLE II: Difference of mean values of E^+ and E^- for 10 participants (value = row - column). Colored cells denote a difference with statistical significance, i.e. $p < 0.05$ in t-test.

E^+	$\boldsymbol{D}_{vel}$	$\boldsymbol{D}_{mean}$	$\boldsymbol{D}_{min}$	$\boldsymbol{D}_{max}$
$\boldsymbol{D}_{pow}$ $\lambda = 2$	0.7329	-1.0504	0.7535	-3.5223
$\boldsymbol{D}_{pow}$ $\lambda = 10$	0.0517	-1.7317	0.0723	-4.2035
E^-	$\boldsymbol{D}_{vel}$	$\boldsymbol{D}_{mean}$	$\boldsymbol{D}_{min}$	$\boldsymbol{D}_{max}$
$\boldsymbol{D}_{pow}$ $\lambda = 2$	-1.5938	-0.1871	-1.5385	0.0554
$\boldsymbol{D}_{pow}$ $\lambda = 10$	-1.4881	-0.0814	-1.4328	0.1611

These results unveil the merit of the proposed approach, which lies in its automatic adjustment property depending on the behaviour of the human. Consequently, there is no need to explicitly tune the damping to find its ideal value for the specific human and/or use-case. It is clear that an adaptation of the damping based on the power results in a significantly better efficiency, as compared to a velocity-based adaptation, particularly for the cooperative manipulation of high inertia objects.

V. Conclusions

In this work a variable admittance control scheme is proposed for providing assistance to a human during the manipulation of a large object with high inertia. The proposed approach is compared to a generic purpose state-of-the-art variable damping approach, via a human-in-the-loop simulation setup. The simulations demonstrate the efficacy of the proposed approach in terms of the reduction of the effort and the enhancement of the user's feeling of control over the task.

References

[1] X. Lamy, F. Colledani, F. Geffard, Y. Measson, and G. Morel, "Achieving efficient and stable comanipulation through adaptation to changes in human arm impedance," in *2009 IEEE International Conference on Robotics and Automation*, 2009, pp. 265–271.

[2] M. Dohring and W. Newman, "The passivity of natural admittance control implementations," in *2003 IEEE International Conference on Robotics and Automation (Cat. No.03CH37422)*, vol. 3, 2003, pp. 3710–3715 vol.3.

[3] A. Lecours, B. Mayer-St-Onge, and C. Gosselin, "Variable admittance control of a four-degree-of-freedom intelligent assist device," in *2012 IEEE international conference on robotics and automation*. IEEE, 2012, pp. 3903–3908.

[4] N. Hogan, "Impedance control: An approach to manipulation: Part i—theory," 1985.

[5] D. E. Whitney, "Force feedback control of manipulator fine motions," 1977.

[6] W. S. Newman, "Stability and performance limits of interaction controllers," 1992.

[7] F. J. Abu-Dakka and M. Saveriano, "Variable impedance control and learning—a review," *Frontiers in Robotics and AI*, vol. 7, p. 177, 2020.

[8] R. Ikeura and H. Inooka, "Variable impedance control of a robot for cooperation with a human," in *Proceedings of 1995 IEEE International Conference on Robotics and Automation*, vol. 3. IEEE, 1995, pp. 3097–3102.

[9] M. Rahman, R. Ikeura, and K. Mizutani, "Investigating the impedance characteristic of human arm for development of robots to co-operate with human operators," in *IEEE SMC'99 Conference Proceedings. 1999 IEEE International Conference on Systems, Man, and Cybernetics (Cat. No. 99CH37028)*, vol. 2. IEEE, 1999, pp. 676–681.

[10] R. Ikeura, T. Moriguchi, and K. Mizutani, "Optimal variable impedance control for a robot and its application to lifting an object with a human," in *Proceedings. 11th IEEE International Workshop on Robot and Human Interactive Communication*. IEEE, 2002, pp. 500–505.

[11] O. M. Al-Jarrah and Y. F. Zheng, "Arm-manipulator coordination for load sharing using variable compliance control," in *Proceedings of International Conference on Robotics and Automation*, vol. 1. IEEE, 1997, pp. 895–900.

[12] V. Duchaine and C. M. Gosselin, "General model of human-robot cooperation using a novel velocity based variable impedance control," in *Second Joint EuroHaptics Conference and Symposium on Haptic Interfaces for Virtual Environment and Teleoperator Systems (WHC'07)*. IEEE, 2007, pp. 446–451.

[13] F. Ficuciello, L. Villani, and B. Siciliano, "Variable impedance control of redundant manipulators for intuitive human–robot physical interaction," *IEEE Transactions on Robotics*, vol. 31, no. 4, pp. 850–863, 2015.

[14] F. Dimeas and N. Aspragathos, "Fuzzy learning variable admittance control for human-robot cooperation," in *2014 IEEE/RSJ International Conference on Intelligent Robots and Systems*. IEEE, 2014, pp. 4770–4775.

[15] S. Grafakos, F. Dimeas, and N. Aspragathos, "Variable admittance control in phri using emg-based arm muscles co-activation," in *2016 IEEE International Conference on Systems, Man, and Cybernetics (SMC)*. IEEE, 2016, pp. 001 900–001 905.

[16] C. Gosselin, T. Laliberté, B. Mayer-St-Onge, S. Foucault, A. Lecours, V. Duchaine, N. Paradis, D. Gao, and R. Menassa, "A friendly beast of burden: A human-assistive robot for handling large payloads," *IEEE Robotics & Automation Magazine*, vol. 20, no. 4, pp. 139–147, 2013.